IET Science, Measurement & Technology

Research Article

IET Journals
The Institution of Engineering and Technology

Comparing frequency-dependent and distributed parameter with lumped losses power cable line models for cable insulation coordination against overvoltages

ISSN 1751-8822
Received on 13th April 2018
Revised 30th July 2018
Accepted on 24th September 2018
doi: 10.1049/iet-smt.2018.5118
www.ietdl.org

Massimo Marzinotto[1] ✉, *Giuseppe Pelliccione*[1]

[1]*TERNA, Via della Marcigliana 911, 00138 Roma, Italy*

✉ *E-mail: massimo.marzinotto@terna.it*

Abstract: Simulations of transients are an obliged step for the insulation coordination of cable lines. Although a frequency-dependent power cable line model better takes into account real conditions since resistive and inductive parameters vary with frequency, a distributed parameter with lumped losses power cable models can be useful to simplify and give higher flexibility to the insulation coordination study. In such a case, a dilemma rises up when a frequency shall be selected for the determination of the cable parameters. In this study, a comparative analysis between the two models has been performed considering a typical configuration layout, i.e. an overvoltage coming from an overhead line and stressing the cable line terminated on a transformer. The overvoltages stressing both cable insulation wall and cable thermoplastic jacket are evaluated using the same system configuration with both frequency-dependent and distributed parameter with lumped losses power cable line models, in the latter case sweeping different frequency values for the determination of the cable parameters. A frequency range that minimise the differences between the overvoltage estimation using the two models is suggested.

1 Introduction

Insulation coordination of power cables under transient conditions implies the study of lightning and switching overvoltages stressing the cable insulation wall [1, 2]. Furthermore, the assessment of the overvoltage stressing the thermoplastic jacket, although not directly involved on the goal of the insulation coordination, shall be evaluated since any damage to the jacket can potentially reduce the life of the cable system [1, 2]. In this respect, the distribution of the overvoltage peak values or the maximum expected overvoltage peak value shall be properly evaluated in order to perform the insulation coordination through a statistic or a deterministic approach, respectively [3–5].

Overvoltages stressing the cable systems mainly arise from internal system electromagnetic transients (switching, faults etc.) and external transients (lightning) usually due to lightning strokes striking overhead lines connected to the cable line. For this reason, it is then necessary to analyse all the possible overvoltages stressing the cable ends. Induced overvoltages arising from a lightning radiated electromagnetic field that directly illuminates the cable system are hardly dangerous for cable insulation at medium voltage level [6] and furthermore they are not relevant for high voltage cable systems. Direct lightning on cables are very difficult to be predicted and furthermore hardly likelihood. Consequently, only overvoltages originated from the terminal stations or along the overhead lines are considered in this paper.

In order to perform a correct evaluation of the transient overvoltage stressing the cable insulation, it is of paramount importance the proper selection of the numerical models to be used for the simulation. As far as cable lines are concerned, different models have been proposed in the literature.

The frequency-dependent models [7–12] take into account the frequency dependence of the resistance and inductance cable matrices and then should be preferred. On the other hand, distributed parameter with lumped losses models [13, 14] are straightforwardly implemented in simulations, since they evaluate resistance and inductance matrices in a single frequency, but some concern can arise in the choice of the frequency to be used for the parameters evaluation that gives results as much as possible similar to those obtained with a frequency-dependent model. This is especially true for cable models, on account of the strong frequency dependence of transformation matrices.

The aim of this paper is to deepen this subject trying to compare the results of two simulations of the same system, one with a frequency-dependent cable line model, and the other with a distributed parameter with the lumped losses cable line model. The latter simulation is repeated at different times varying each time the frequency for the evaluation of the cable parameters. Each simulation with the constant-parameter model is then compared with the results obtained from the frequency-dependent model. A quantitative comparison has been reserved to the peak values and a qualitative comparison to the shape of the waves. Special attention has been given to the peak values since in the insulation coordination approach such values mainly drive the goal.

2 Analysed configurations

A configuration typically considered in the studies of insulation coordination of cable line systems [1, 2, 5, 15] has been taken into account. The configuration is reported in Fig. 1 in which a cable line is in between an overhead line of infinite length and a transformer (de facto an open line end under a transient point of view). This configuration is the one that represents the worst condition for the cable line insulation coordination [1, 2, 5, 15, 16]. The overvoltage is considered coming from the overhead line and stressing the cable line. No surge arrester is considered. Cable screen is earthed at both cable ends only considering an earthing surge impedance of 10 and 1 Ω at the transition overhead to cable end (sending end) and at the transformer end (receiving end), respectively. Although in the real world, there could be some screen earthing connections along the cable line, earthing the screen at the cable line ends only represents a conservative condition [1, 2, 5].

No flashovers are considered on the cable terminations or on overhead sections external to the cable system in order not to

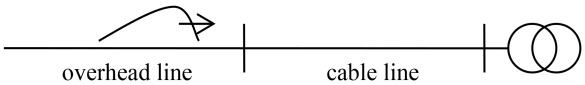

Fig. 1 *Sketch of the system configuration considered in the simulation*

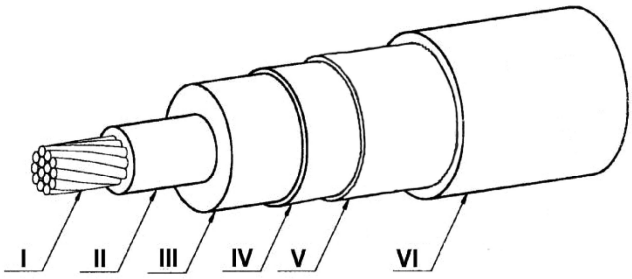

Fig. 2 *Typical XLPE cable formation: (I) conductor, (II) inner semiconductive layer, (III) insulation wall, (IV) outer semiconductive layer, (V) metallic continuous screen, (VI) thermoplastic jacket*

Table 1 150 and 400 kV cable characteristics and formation

	150 kV cable		
conductor cross section	1600 mm^2	conductor radius	26 mm
inner semicon thickness	2 mm	inner semicon ε	1000
insulation thickness	20 mm	insulation ε	2.6
outer semicon thickness	1 mm	outer semicon ε	1000
inner semicon resist.	10 Ωm	outer semicon resist.	10 Ωm
insulation tan δ	0.4×10^{-3}	insulation type	XLPE
screen cross section	210 mm^2	screen type	sheath
conductor material	aluminium	screen material	aluminium
jacket thickness	5 mm	Jacket ε	2.3
jacket material	PE	soil resistivity	100 Ωm
disposition type	flat	burying depth	1.3 m
	400 kV cable		
conductor cross section	2500 mm^2	conductor radius	28 mm
inner semicon thickness	2 mm	inner semicon E	1000
insulation thickness	28 mm	insulation ε	2.3
outer semicon thickness	2 mm	outer semicon E	1000
inner semicon resistivity	10 Ωm	outer semicon resistivity	10 Ωm
insulation tan δ	0.4×10^{-3}	insulation type	XLPE
screen cross section	393 mm^2	screen type	sheath
conductor material	Copper	screen material	aluminium
jacket thickness	5 mm	jacket ε	2.3
jacket material	PE	soil resistivity	100 Ωm
disposition type	Flat	burying depth	1.3 m

introduce a non-linearity. Conductor-to-screen and screen-to-ground overvoltages at both cable ends are considered.

Two cable ratings have been selected for the simulation: 150 kV – 1600 mm^2 aluminium conductor cross section and 400 kV – 2500 mm^2 copper conductor cross section. Characteristics and formation (see Fig. 2) of the two cable ratings are reported in Table 1.

The conductor dispositions of the overhead line are those usually adopted for the single circuit 150 kV level (single conductor – triangle disposition) and the single circuit 400 kV level (three-bundle conductor – flat disposition) that for the sake of brevity are not further illustrated. The transformer has been represented with a lumped resistance of 5 kΩ [16].

3 Cable line models and comparison

The MATLAB© environment has been used for the numerical simulation.

The frequency-dependent cable model has been developed through the fast Fourier transform (FFT). For the sake of brevity, in this paper, such model is recalled as 'Fourier' model.

The distributed parameter with lumped losses cable model is based on the Bergeron's travelling wave method used by the Electromagnetic Transient Program [13, 14]. For the sake of brevity, in this paper, such model is recalled as 'Bergeron' model. For this model, a maximum cable length of 1 km has been considered. Consequently, for the representation of cable lengths higher than 1 km, more than one element has been connected in series in order to have a sequence of equal length elements, e.g. a cable line length of 3.2 km is represented as a segmented line composed of four elements each 0.8 km long.

In order to compare the outputs from the above mentioned simulations, an error (1) has been introduced as the difference between the absolute peak value of the overvoltage at a specific location between the simulation using the Fourier model and the simulation using the Bergeron model. Such error ε is frequency dependent since the outputs of the simulations using the Bergeron model are a set of simulations, each one performed with a different frequency for the evaluation of the cable parameters

$$\varepsilon(f) = \frac{V_{\mathrm{B}}(f) - V_{\mathrm{F}}}{V_{\mathrm{F}}} \tag{1}$$

where V_{F} and V_{B} are the voltage peak values at specific locations with the simulations using Fourier and Bergeron models, respectively. The overvoltages are evaluated at the transition from overhead line to cable (sending end) and at the cable transformer end (receiving end). At such locations, the maximum overvoltages are expected if no surge arresters are installed at cable end(s).

The analysis on finding the frequency for the Bergeron model that reduces at a minimum the error (1) is performed separately for the conductor-to-screen propagation mode and the screen-to-ground propagation mode. As illustrated in the following section, the frequency that gives the minimum error ε is the same that gives

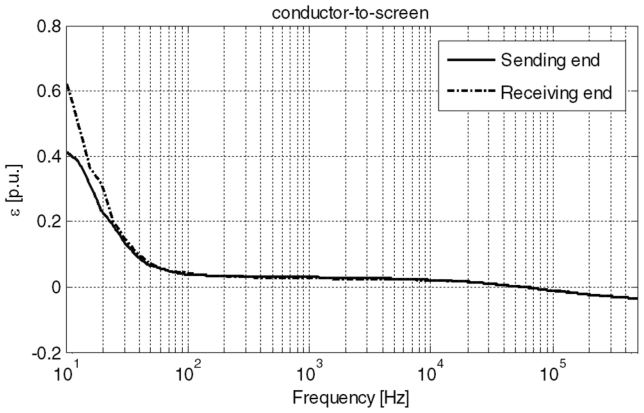

Fig. 3 *Conductor-to screen error ε versus frequency at sending end and receiving end of a 150 kV cable line with a stressing 1.2/50 μs standard waveshape from the overhead line*

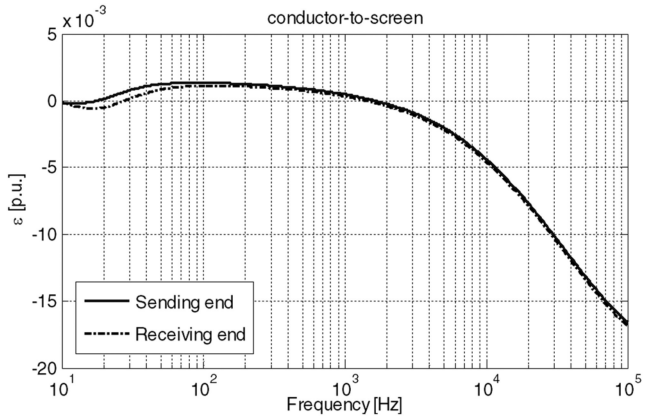

Fig. 4 *Conductor-to screen error ε versus frequency at sending end and receiving end of a 150 kV cable line with a stressing 250/2500 μs standard waveshape from the overhead line*

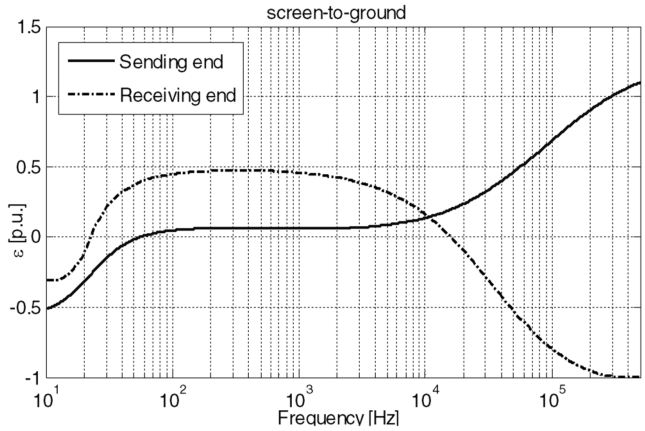

Fig. 5 *Screen-to ground error ε versus frequency at sending end and receiving end of a 150 kV cable line with a stressing 1.2/50 μs standard waveshape from the overhead line*

very similar waveshapes with the Fourier model and the Bergeron model. A frequency that reduces the error (1) for both propagation modes is suggested. The simulation outcomes highlight that the range of frequencies that minimises the error ε is substantially independent to the overhead line configuration, cable insulation level (cable rating), load condition at the receiving end and screen earthing at both cable ends, but it strongly depends on the overvoltage waveshape only.

The simulations are performed considering the standard lightning voltage waveshape (1.2/50 μs wave) and the standard switching voltage waveshape (250/2500 μs wave) [17] in order to consider both fast and a slow front overvoltages, respectively. The waveshapes have been simulated by the Heidler function [18, 19] with adequately selected parameters, which is more realistic than the typical double exponential function. In fact, the first derivative of Heidler function is zero at the foot of the wave in spite of the double exponential wave.

The evaluation of the error has been undertaken in the frequency range 10 Hz and 500 kHz. It is important to remind that the well-known models used for the ground return, i.e. Carson [20] for overhead lines and Pollaczek [21, 22] for cable lines, lose their validity for frequencies higher than 1 MHz since they do not take into account the displacement currents [23]. On the other hand, considering the typical overvoltage waveshapes arising from lightning events in power systems, the frequency spectrum reduces practically to zero at a frequency of 500 kHz for the standard 1.2/50 μs wave.

4 Discussion of results

Fig. 3 shows the error (1) for the voltage conductor-to-screen mode versus frequency for a 1.2/50 μs waveshape coming from the overhead line and stressing the cable line. This figure highlights that the error is about zero in the frequency range of 40–70 kHz. The error (1) at both sending and receiving ends are practically the same, except for frequency values below about 100 Hz. For frequency lower than 1 kHz the error increases as the frequency decreases. For frequency values above 80 kHz, the error becomes negative turning the Bergeron model non-conservative in respect of the Fourier model.

Fig. 4 shows the error (1) on the voltage conductor-to-screen mode versus frequency for a 250/2500 μs waveshape coming from the overhead line and stressing the cable line. This figure highlights that the error is around zero in the frequency range of 0.1–2 kHz. There are no differences between sending and receiving ends for the whole frequency range considered except for frequency values below about 100 Hz and above 100 kHz. For frequency values above about 2 kHz, the error becomes negative turning the Bergeron model non-conservative in respect of the Fourier model.

Fig. 5 shows the variation of the error (1) for the screen-to-ground mode at both sending and receiving ends when the stressing overvoltage travelling from the overhead line is a 1.2/50 μs waveshape. In such a case since the overvoltage from the overhead line directly stresses the cable insulation wall and since no flashover occurs, the overvoltage travelling the screen-to-ground mode is due to the coupling with the overvoltage travelling on the conductor-to-screen mode. The error function (1) versus frequency at the sending end is completely different to that at the receiving end, on the contrary to what observed for the conductor-to-screen mode (Figs. 3 and 4). The error function (1) at sending end is positive for frequencies higher than 50 Hz and is quite constant around 6% from 100 Hz to 2–3 kHz, increases at a frequency higher than 3 kHz. Considering the receiving end, the error function (1) passes from −30 to 45% from 10 to 100 Hz and crosses zero around 25 Hz. From 100 Hz to 2 kHz is quite constant (around 45%) and for higher frequencies starts to decrease crossing zero around 16 kHz. This different behaviour of the error function (1) for the sending and receiving ends makes difficult the choice of the frequency that better reduces the error between the two models. The best frequency value is around 11 kHz where the error is in the order of 15%.

Fig. 6 shows the values of the error function (1) for the screen-to-ground propagation mode at both sending and receiving ends when the overvoltage travelling from the overhead line and stressing the cable line has a 250/2500 μs standard waveshape. In this case, except for frequency lower than 20 Hz and larger than 1 kHz, the error function both at the sending and at the receiving ends is very low (ranging from 0 to 5%). The error function (1) at the sending end starts to increase for frequency above 3 kHz, while at the receiving end crosses zero around 800 Hz and then becomes more and more negative as far as the frequency increases.

Table 2 reports the best frequency range values that reduce the error function (1) to a minimum considering both the standard overvoltage waveshapes (1.2/50 and 250/2500 μs) for the two

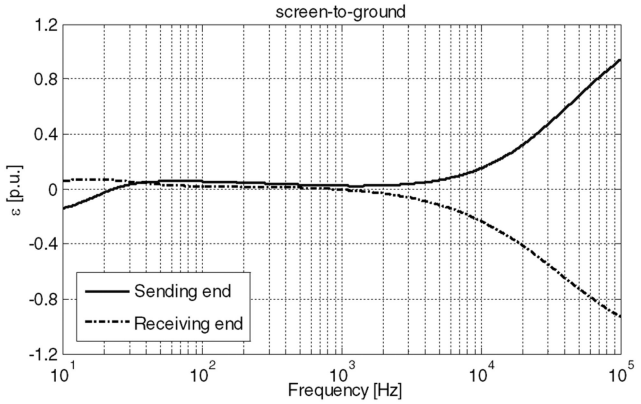

Fig. 6 *Screen-to ground error ε versus frequency at sending end and receiving end of a 150 kV cable line with a stressing 250/2500 μs standard waveshape from the overhead line*

Table 2 Summary of the results for the fast (1.2/50 μs) and slow (250/2500 μs) stressing overvoltages: the frequency ranges to reduce the error function below ±0.5% for the two modes of propagation and at the sending and receiving ends

		1.2/50 μs waveshape		
		Conductor-to screen mode		Screen-to-ground mode
	Sending end	Receiving end	Sending end	Receiving end
frequency	from 57 to 58 kHz	from 57 to 58 kHz	from 54 to 58 Hz	from 15.6 to 16.0 kHz
ε	<±0.5%	<±0.5%	<±0.5%	<±0.5%
		250/2500 μs waveshape		
		Conductor-to screen mode		Screen-to-ground mode
	Sending end	Receiving end	Sending end	Receiving end
frequency	from 1.0 to 2.2 kHz	from 1.0 to 2.2 kHz	from 23 to 24 Hz	from 0.65 to 1 kHz
ε	<±0.5%	<±0.5%	<±0.5%	<±0.5%

Table 3 Summary of the results for the fast (1.2/50 μs) and slow (250/2500 μs) stressing overvoltages: a common frequency range for both sending and receiving ends to minimise the error

		1.2/50 μs waveshape	
		Conductor-to screen mode	Screen-to-ground mode
frequency	from 43 to 57 kHz	from 10.3 to 11.1 kHz	
ε	<0.5%	from 12 to 15%	
		250/2500 μs waveshape	
		Conductor-to screen mode	Screen-to-ground mode
frequency	from 1.0 to 1.4 kHz	from 23 to 820 Hz	
ε	<0.5%	from 0 to 7%	

modes of propagation (conductor-to-screen and screen-to-ground) at the sending and receiving ends.

In general, a range of frequency for each waveshape, for each mode of propagation and for both sending and receiving ends is not useful under a practical point of view. Consequently, a selection of a single frequency range per overvoltage waveshapes and per mode of propagation shall be addressed, bearing in mind that in such a case a higher error shall be accepted. For the reasons illustrated in the previous section, it is important that the error is positive in order to be conservative in the estimation of the overvoltage. Table 3 reports the results considering this goal.

If one frequency range only for both propagation modes is selected, in the case of the 1.2/50 μs waveshape this range is between 10 and 11 kHz and the error (1) varies between 2.1 and 2.2% and between 15 and 16% for the conductor-to-screen mode and for the screen-to-ground mode, respectively. While for the 250/2500 μs wave shape this range is between 600 and 800 Hz and the error (1) is equal to 0.1% for the conductor-to-screen mode and around 3% for the screen-to-ground mode. Considering real conditions, the conductor-to-screen mode overvoltage is usually at least one order of magnitude higher than the screen-to-ground mode, usually hundreds of kVs against some kV [1, 2]. Cable reliability under stressing overvoltages is primarily focused on the cable insulation wall [24]. Thermoplastic jacket faults (damages, grazes, punctures etc.) do not impede the operation of the cable systems in spite of a fault in the insulation wall. If the current on the jacket fault location is negligible (high resistance fault) and does not exceed a safety threshold, the cable can be maintained in operation at full or reduced current rating under a proper screen current supervision [25] postponing in this way the jacket repair at a later stage during the forecasted maintenance spell. For these reasons, a lower error is allowed for the conductor-to-screen mode than for the screen-to-ground mode. Table 4 shows the suggested frequency ranges to be adopted for the Bergeron parameters and the relevant errors for each propagation mode for the two analysed standard overvoltage waveshapes.

The above analysis performed with the 150 kV cable line can be considered valid also for the 400 kV cable line since the simulation outcomes are very similar and for the sake of brevity are omitted here.

With the aim to illustrate some specific case, in the following the results of the simulations using both the Fourier and the Bergeron models are reported.

Figs. 7 and 8 show the overvoltage at the sending end of a 150 kV line 1 km long on the conductor-to-screen mode and on the screen-to-ground mode, respectively when the cable model has both the Fourier and Bergeron models. The stressing overvoltage is the 1.2/50 μs standard waveshape. The cable parameters of the Bergeron model have been evaluated with a frequency of 11 kHz. Such figure highlights that the Fourier model has a smoother waveshape especially on the tail, while the Bergeron model has a larger damping effect on the tail (see Fig. 8). In both cases, the

Table 4 Suggested frequencies for each standard overvoltage waveshape and relevant error for the conductor-to-screen and screen-to-ground modes

		1.2/50 μs waveshape		
			Conductor-to screen mode	Screen-to-ground mode
frequency		from 10 to 11 kHz		
ε	from 2.1 to 2.2%		from 15 to 16%	
		250/2500 μs waveshape		
			Conductor-to screen mode	Screen-to-ground mode
frequency		from 600 to 800 Hz		
ε	<0.1%		≅3%	

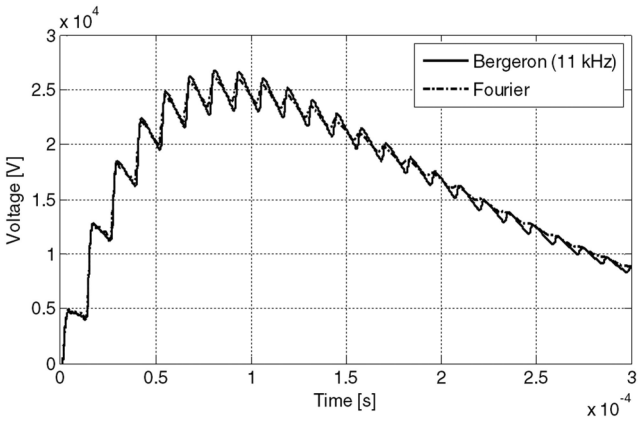

Fig. 7 *Conductor-to-screen overvoltage at the sending end of a 150 kV cable line 1 km long for a 1.2/50 μs 100 kV peak impulsive wave coming from the overhead line conductor. Both frequency-dependent (Fourier) and distributed parameter with lumped losses (Bergeron) cable line models. The parameters of the Bergeron model are evaluated with a frequency of 11 kHz*

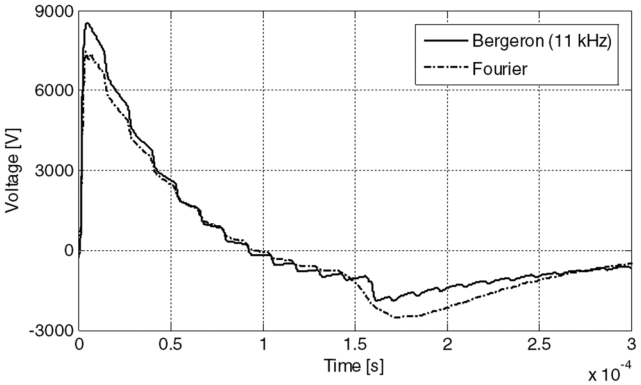

Fig. 8 *Screen-to-ground induced overvoltage at the sending end of a 150 kV cable line 1 km long for a 1.2/50 μs 100 kV peak impulsive wave coming from the overhead line conductor. Both frequency-dependent (Fourier) and distributed parameter with lumped losses (Bergeron) cable line models. The parameters of the Bergeron model are evaluated with a frequency of 11 kHz*

Bergeron model gives more conservative results than the Fourier model. In particular, Fig. 8 shows that the error, although in excess of about 15%, it can be deemed acceptable: practically such 15% excess does not substantially change the countermeasures to be adopted to reduce the risk of cable jacket puncture.

Interesting is to note the simulation results reported in Figs. 9 and 10 where the same 150 kV cable line of Figs. 7 and 8 is reported but with a cable line length of 5 km. As already mentioned above, for the Bergeron simulation, five models representing a cable length section of 1 km each have been connected in series. The effect of such a series connection can be revealed on the simulation outcomes: between each reflection from the cable end, five oscillations can be counted on both the conductor-to-screen and the screen-to-ground modes. Such oscillations contribute to give rough waveshapes but they do not alter the absolute peak value of the overvoltage. Simulations with a single section 5 km long have also been performed, but the final results give a higher

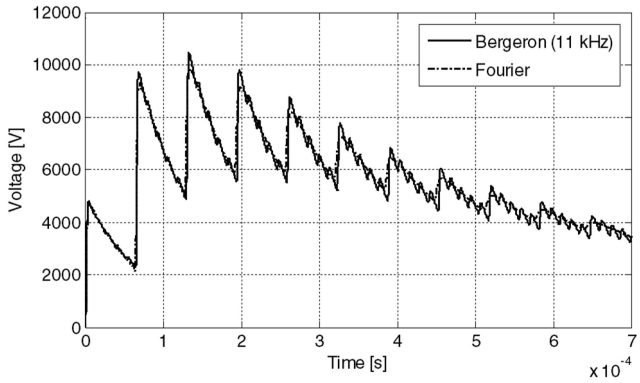

Fig. 9 *Conductor-to-screen overvoltage at the sending end of a 150 kV cable line 5 km long for a 1.2/50 μs 100 kV peak impulsive wave coming from the overhead line conductor. Both frequency-dependent (Fourier) and distributed parameter with lumped losses (Bergeron) cable line models. The parameters of the Bergeron model are evaluated with a frequency of 11 kHz*

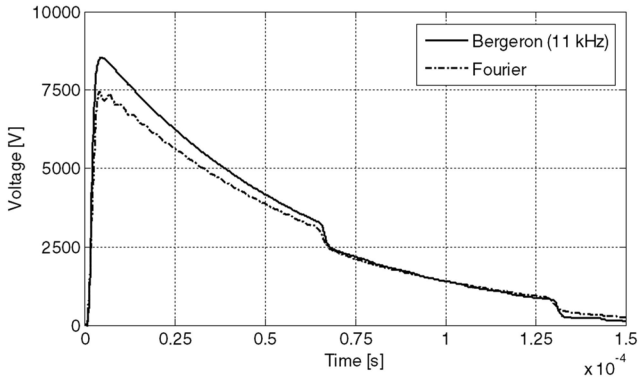

Fig. 10 *Screen-to-ground induced overvoltage at the sending end of a 150 kV cable line 5 km long for a 1.2/50 μs 100 kV peak impulsive wave coming from the overhead line conductor. Both frequency-dependent (Fourier) and distributed parameter with lumped losses (Bergeron) cable line models. The parameters of the Bergeron model are evaluated with a frequency of 11 kHz*

error than simulations performed with a segmented line composed of five sections each 1 km long, due to the larger lumped losses. The cascade of five cable sections allows, indeed, a better losses distribution along the line. Using cable sections with a length lower than 1 km does not contribute to reducing the error substantially. Consequently, in the simulation with the Bergeron model, more sections series connected are recommended for cable length larger than 1 km.

The same system analysed in Figs. 9 and 10 is further analysed with a 250/2500 μs standard waveshape and the results of the simulations are reported in Figs. 11 and 12 for the conductor-to-screen and the screen-to-ground modes, respectively. In this case, the frequency used for the estimation of the Bergeron model parameters has been selected equal to 800 Hz in line with the values reported in Table 4. In such a case, for the reduced errors value, the two waveshapes (Fourier and Bergeron) for both the conductor-to-screen and the screen-to-ground modes are quite the same. The higher damping effect on the tail of the Bergeron model,

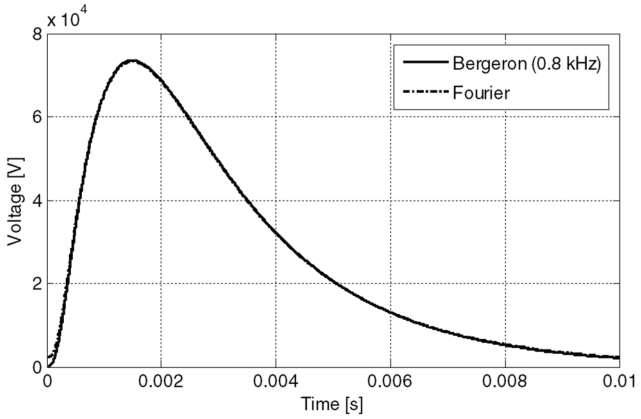

Fig. 11 *Conductor-to-screen overvoltage at the sending end of a 150 kV cable line 5 km long for a 250/2500 μs 100 kV peak impulsive wave coming from the overhead line conductor. Both frequency-dependent (Fourier) and distributed parameter with lumped losses (Bergeron) cable line models. The parameters of the Bergeron model are evaluated with a frequency of 800 Hz*

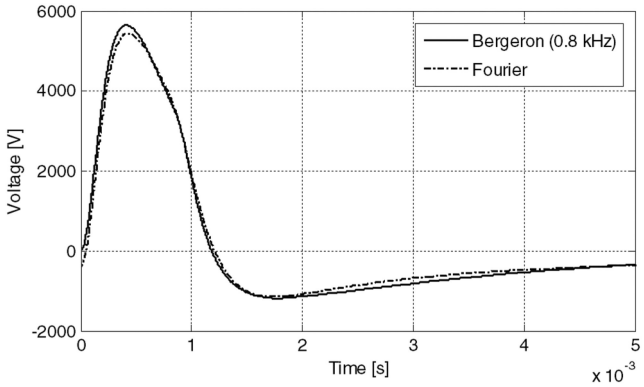

Fig. 12 *Screen-to-ground induced overvoltage at the sending end of a 150 kV cable line 5 km long for a 250/2500 μs 100 kV peak impulsive wave coming from the overhead line conductor. Both frequency-dependent (Fourier) and distributed parameter with lumped losses (Bergeron) cable line models. The parameters of the Bergeron model are evaluated with a frequency of 800 Hz*

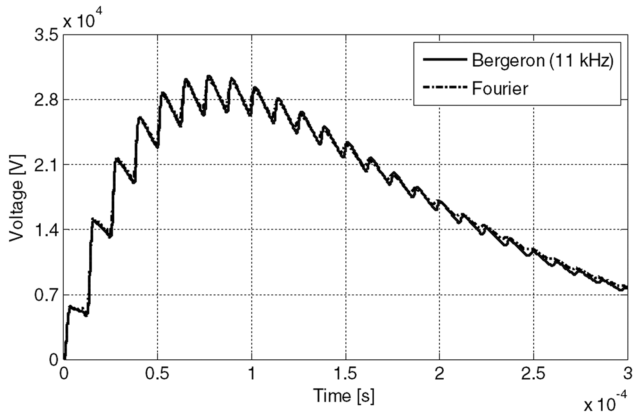

Fig. 13 *Conductor-to-screen overvoltage at the sending end of a 400 kV cable line 1 km long for a 1.2/50 μs 100 kV peak impulsive wave coming from the overhead line conductor. Both frequency-dependent (Fourier) and distributed parameter with lumped losses (Bergeron) cable line models. The parameters of the Bergeron model are evaluated with a frequency of 11 kHz*

typical of the 1.2/50 μs waveshape, as shown above, disappears in this case. The oscillations due to the sequence of five cable section of 1 km each connected in series in the time-domain simulation disappears due to the lower front steepness of the 250/2500 μs wave in respect of the 1.2/50 μs wave.

In Figs. 13 and 14, the conductor-to-screen waveshapes at the sending and at the receiving ends of a 1 km – 400 kV cable line

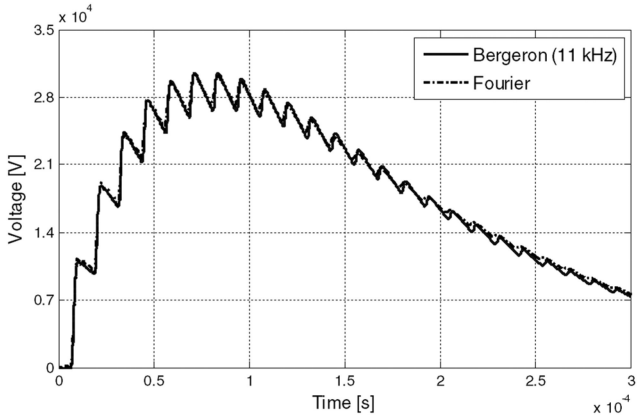

Fig. 14 *Conductor-to-screen overvoltage at the receiving end of a 400 kV cable line 1 km long for a 1.2/50 μs 100 kV peak impulsive wave coming from the overhead line conductor. Both frequency-dependent (Fourier) and distributed parameter with lumped losses (Bergeron) cable line models. The parameters of the Bergeron model are evaluated with a frequency of 11 kHz*

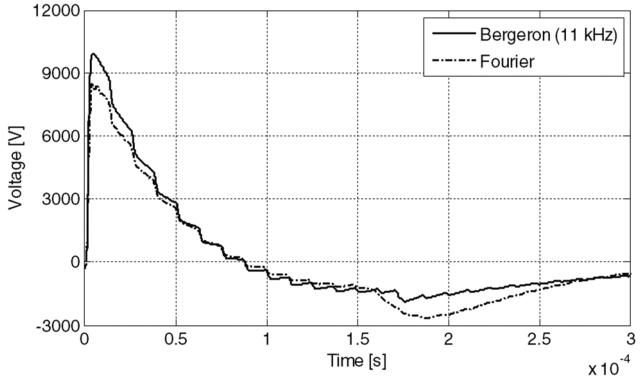

Fig. 15 *Screen-to-ground induced overvoltage at the sending end of a 400 kV cable line 1 km long for a 1.2/50 μs 100 kV peak impulsive wave coming from the overhead line conductor. Both frequency-dependent (Fourier) and distributed parameter with lumped losses (Bergeron) cable line models. The parameters of the Bergeron model are evaluated with a frequency of 11 kHz*

stressed with a 1.2/50 μs standard waveshape are reported. Comparing such figures with Fig. 7, it can be stated that they are very similar except for the peak value. This fact highlights how the analysis extended to the 400 kV system does not give different qualitative results. Furthermore, under a qualitative point of view, the overhead line has a very negligible impact as well.

As far as the screen-to-ground overvoltage waveshapes of the same 1 km long – 400 kV case considered above are concerned, Figs. 15 and 16 show the situation at the sending and receiving ends, respectively. Again, under a qualitative point of view, the situation does not differ so much from the same 150 kV case. The excess in the evaluation of the peak value, i.e. about 2 kV (overvoltage peak 8 kV for the Fourier model against about 10 kV for the Bergeron model) at the sending end and about 0.6 kV (overvoltage peak 3.8 kV for the Fourier model against the 4.4 kV for the Bergeron model) at the receiving end, has not a practical impact on the countermeasures to be adopted to reduce the risk of jacket puncture.

From the same figures, it can be highlighted that, as already mentioned for the previous cases, a stronger damping occurs on the tail for the Bergeron model. In Fig. 16, it can be observed how the Fourier model gives rise to a much gentle waveshape in respect of the Bergeron model in which has a very steep front and a jagged tail in line with what already highlighted above.

5 Conclusion

The paper has compared the results of two simulations of the same system, one with a frequency-dependent cable line model, and the other with a distributed parameter with the lumped losses cable line

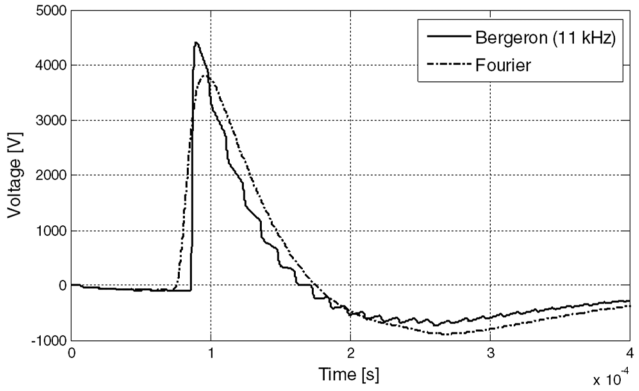

Fig. 16 *Screen-to-ground induced overvoltage at the receiving end of a 400 kV cable line 1 km long for a 1.2/50 μs 100 kV peak impulsive wave coming from the overhead line conductor. Both frequency-dependent (Fourier) and distributed parameter with lumped losses (Bergeron) cable line models. The parameters of the Bergeron model are evaluated with a frequency of 11 kHz*

model. It has been considered a typical situation occurring in practice where the cable line is in between an overhead line and a transformer. The analysis has been focused to the overvoltages at both the sending and receiving ends and for both the conductor-to-screen and the screen-to-ground modes of propagation. The overvoltage has been considered coming from the overhead line and impinging the transition overhead to the cable end.

The difference in terms of peak values, between the frequency-dependent and the distributed parameter with lumped losses models, becomes small and seldom negligible if a proper frequency is selected for the determination of the parameters in the latter model. Such frequency is influenced only by the overvoltage waveshape coming from the overhead line.

The frequency suggested for the estimation of the frequency-dependent cable parameters (R and L through Schelkunoff theory) to be used in the distributed parameter with lumped losses models shall fall within 10–11 kHz range if the cable stressing overvoltage has a 1.2/50 μs standard waveshape, while shall fall in the range of 600–800 Hz for a 250/2500 μs standard waveshape. With the suggested frequency values, the distributed parameter with lumped losses models gives very similar and conservative results in respect of the frequency-dependent models. Under a qualitative point of view, the waves with the two models are very similar. In particular, as far as a fast front overvoltage stresses the cable line, the results obtained with the distributed parameter with lumped losses models give rise to lightly steeper fronts and lightly jagged tails if compared with the results obtained through the frequency-dependent models in which the wave shape are always gentler. On the other hand, when a slow front overvoltage stresses the cable line, the waveshapes from the two models can be quite overlapped.

The selection of a distributed parameter with the lumped losses cable model, with a proper frequency in the estimation of its parameters, can be useful to simplify and give higher flexibility to the insulation coordination study, whenever the simulation is performed considering incoming overvoltages with standard waveshapes (1.2/50 and 250/2500 μs, respectively) and a typical cable configuration.

6 References

[1] Marzinotto, M.: 'Relationship between impinging and stressing overvoltages statistical distributions in power cable lines'. IEEE Power Tech 2007, Lausanne, Switzerland, 1–5 July 2007

[2] Marzinotto, M., Mazzetti, C.: 'Overvoltage attenuation in power cable lines – a simplified estimation method', *Electr. Power Syst. Res.*, 2010, **80**, (5), pp. 506–513

[3] Barthold, L.O., Paris, L.: 'The probabilistic approach to insulation coordination', *Electra*, 1970, **13**, pp. 41–58

[4] Paris, L.: 'Insulation coordination'. High Voltage Engineering Research Proc., ENEL R&D Management, Italy, 1970

[5] Marzinotto, M.: 'Insulation coordination of extruded power cable lines'. PhD Thesis, Roma, Italy, September 2006, 376p. Padis Ed. – pub. no 1148369693_31587

[6] Borghetti, A., Marzinotto, M., Mazzetti, C., *et al.*: 'Insulation coordination of MV cables against lightning-induced overvoltages generated by LEMP-coupled overhead lines'. Proc. of 28th Int. Conf. on Lightning Protection ICLP 2006, Kanazawa, Japan, 18–22 September 2006

[7] Marti, J.R.: 'The problem of frequency dependence in transmission line modelling'. PhD Dissertation, University of British Columbia, Canada, 1981

[8] Marti, J.R.: 'Accurate modelling of frequency-dependent transmission lines in electromagnetic transient simulations', *IEEE Trans. Power Appar. Syst.*, 1982, **PAS-101**, (1), pp. 147–155

[9] Bickford, J.P., Mullineux, N., Reed, J.R.: '*Computation of power-system transients*' (Peter Peregrinus Ltd., London, 1980)

[10] Semlyen, A., Dabuleanu, A.: 'Fast and accurate switching transient calculations on transmission lines with ground return using recursive convolutions', *IEEE Trans. Power Appar. Syst.*, 1975, **PAS-94**, (2), pp. 561–571

[11] Noda, T., Nagaoka, N., Ametani, A.: 'Phase domain modelling of frequency-dependent transmission lines by means of an ARMA model', *IEEE Trans. Power Deliv.*, 1996, **11**, (1), pp. 401–411

[12] Morched, A., Gustavsen, B., Tartibi, M.: 'A universal model for accurate calculation of electromagnetic transients on overhead lines and underground cables', *IEEE Trans. Power Deliv.*, 1999, **14**, (3), pp. 1032–1038

[13] Bergeron, L.: '*Du coup de bélier en hydraulique au coup de foudre en électricité*' (Dunod, Paris, 1950)

[14] Dommel, H.: 'Digital computer solution of electromagnetic transients in single and multiple networks', *IEEE Trans. Power Appar. Syst.*, 1969, **PAS-88**, (4), pp. 388–399

[15] Marzinotto, M., Mazzetti, C., Schiaffino, P.: 'Statistical approach to the insulation coordination of medium and high voltage cable lines'. Proc. of IEEE Power Tech 2005, St. Petersburg, Russia, 27–30 June 2005

[16] Morello, A.: 'Extra high voltage cables and impulse reflections', *L'Elettrotecnica*, 1956, **43**, (12) (in italian), pp. 674–689

[17] IEC 60060-1: 'High-voltage test techniques part 1: general definitions and test requirements', IEC/TC 42 High-voltage testing techniques, September 2010

[18] Heidler, F., Cvetić, J.M., Stanić, B.V.: 'Calculation of lightning current parameters', *IEEE Trans. Power Deliv.*, 1999, **14**, (2)

[19] Heidler, F., Wieisenger, J., Zischank, W.: 'Lightning currents measured at a telecommunication tower from 1992 to 1998'. Proc. of the 14th Int. Symp. on Electromagnetic Compatibility, Zurich, Switzerland, 2001

[20] Carson, J.R.: 'Wave propagation in overhead wires with ground return', *Bell Syst. Tech. J.*, 1926, **5**, pp. 539–554

[21] Pollaczek, F.: 'Sur le champ produit par un conducteur simple infiniment long parcouru par courant alternatif', *Rev. Gen. Electr.*, 1931, **29**, pp. 851–867

[22] Wedepohl, L.M., Wilcox, D.J.: 'Transient analysis of underground power-transmission systems', *ibid*, 1973, **120**, (2), pp. 253–260

[23] Ametani, A.: 'A general formulation of impedance and admittance of cables', *IEEE Trans. Power Appar. Syst.*, 1980, **PAS-99**, (3), pp. 189–197

[24] Mazzanti, M., Marzinotto, M.: '*Extruded cables for high voltage direct current transmission – advances in research and development*' (IEEE Series/ Wiley, New York, 2013)

[25] Marzinotto, M., Mazzanti, G.: 'The feasibility of cable sheath fault detection by monitoring sheath-to-ground currents at the ends of cross-bonding sections', *IEEE Trans. Ind. Appl.*, 2015, **51**, (6), pp. 5376–5384

[26] Schelkunoff, S.A.: 'The electromagnetic theory of coaxial transmission lines and cylindrical shields', *Bell Syst. Tech. J.*, 1934, **13**, pp. 532–579

[27] Ametani, A., Miyamoto, Y., Nagaoka, N.: 'Semiconducting layer impedance and its effect on cable wave-propagation and transient characteristic', *IEEE Trans. Power Deliv.*, 2004, **19**, (4), pp. 1523–1531

[28] Amekawa, N., Nagaoka, N., Baba, Y., *et al.*: 'Derivation of semiconducting layer impedance and its effect on cable wave propagation and transient characteristics', *IEE Proc., Gener. Transm. Distrib.*, 2003, **150**, (4), pp. 434–440

[29] Baba, Y., Tanabe, N., Nagaoks, N., *et al.*: 'Transient analysis of a cable with low conducting layers by a finite time-domain method', *IEEE Trans. Electromagn. Compat.*, 2004, **46**, (3), pp. 488–498

[30] Marzinotto, M., Mazzetti, C.: 'Propagation of transients in extruded MV and HV cables considering typical thickness and resistivity values of commercial semiconductive compounds'. Proc. of the Int. Power System Transients Conf. IPST 2007, Lyon, France, 4–7 June 2007

7 Appendix

7.1 'Fourier' model

For a multi-phase transmission line, the telegrapher's equations in the frequency domain take the form of two matrix equations:

$$\frac{\mathrm{d}^2|\boldsymbol{V}|}{\mathrm{d}z^2} = [\boldsymbol{Z}][\boldsymbol{Y}] \cdot |\boldsymbol{V}| \tag{2}$$

$$\frac{d^2|\boldsymbol{I}|}{dz^2} = [\boldsymbol{Y}][\boldsymbol{Z}] \cdot |\boldsymbol{I}| \tag{3}$$

where $|\boldsymbol{V}|$ and $|\boldsymbol{I}|$ are the vectors of voltages and currents at a distance z along the line, respectively. $[\boldsymbol{Z}]$ and $[\boldsymbol{Y}]$ are the square matrices of impedance and admittance, respectively.

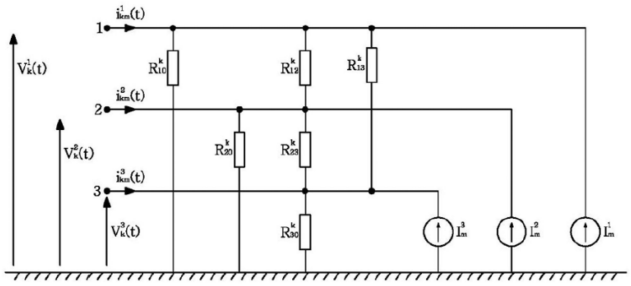

Fig. 17 *Model of a lossless multi-phase line*

For an underground single-core coaxial cable, the component impedances and admittances per unit length are given by the Schelkunoff theory [23, 26] properly modified to take into account the semiconductive layers, always used in power cables from 6 kV and above. In particular, impedance and admittance of such layers have been considered taking into account the developments performed by Ametani *et al.* [27–30]. The ground return has been considered using the Wedepohl–Wilcox's approximated Pollaczek formula [21, 22]. The component impedances and admittances per unit length are frequency-dependent.

With eigenvalue theory, it becomes possible to transform the coupled equations from phase quantities to modal quantities in such a way that the associated matrices become diagonal. These decoupled equations can then be solved as if they were single-phase equations

$$\frac{\mathrm{d}^2|\boldsymbol{V}_m|}{\mathrm{d}z^2} = [\boldsymbol{T}_V]^{-1}[\boldsymbol{Z}][\boldsymbol{Y}][\boldsymbol{T}_V] \cdot |\boldsymbol{V}_m| \tag{4}$$

$$\frac{\mathrm{d}^2|\boldsymbol{I}_m|}{\mathrm{d}z^2} = [\boldsymbol{T}_I]^{-1}[\boldsymbol{Y}][\boldsymbol{Z}][\boldsymbol{T}_I] \cdot |\boldsymbol{I}_m| \tag{5}$$

where $|\boldsymbol{V}_m|$ and $|\boldsymbol{I}_m|$ are the vectors of modal voltages and currents at a distance z along the line, respectively. $[\boldsymbol{T}_V]$ and $[\boldsymbol{T}_I]$ are the square matrices of the eigenvectors.

Using the Fourier transform, the incoming overvoltage can be represented as a group of sine waves, each with a specified amplitude and phase shift. If a sine wave at a given frequency is injected into the modal system, if the system is linear, it will respond at that same frequency with a certain magnitude and a certain phase angle relative to the input.

The determination of the time domain response from its frequency domain expression is made using the inverse Fourier transform.

7.2 'Bergeron' model

For a lossless multi-phase transmission line, the telegrapher's equations in the time domain take the form of two matrix equations:

$$\frac{\mathrm{d}^2|\boldsymbol{V}|}{\mathrm{d}z^2} = [\boldsymbol{L}][\boldsymbol{C}] \cdot \frac{\mathrm{d}^2|\boldsymbol{V}|}{\mathrm{d}t^2} \tag{6}$$

$$\frac{\mathrm{d}^2|\boldsymbol{I}|}{\mathrm{d}z^2} = [\boldsymbol{C}][\boldsymbol{L}] \cdot \frac{\mathrm{d}^2|\boldsymbol{I}|}{\mathrm{d}t^2} \tag{7}$$

where $|\boldsymbol{V}|$ and $|\boldsymbol{I}|$ are the vectors of voltages and currents at time t and distance z along the line, respectively. $[\boldsymbol{L}]$ and $[\boldsymbol{C}]$ are the square matrices of inductance and capacitance, respectively.

For an underground single-core coaxial cable, the component impedances and admittances per unit length are given by the Schelkunoff theory [23, 26] properly modified to take into account the semiconductive layers [27–30]. The ground return has been considered using the Wedepohl–Wilcox's approximated Pollaczek formula [21, 22].

With eigenvalue theory, it becomes possible to transform the coupled equations from phase quantities to modal quantities in such a way that the associated matrices become diagonal

$$\frac{\mathrm{d}^2|\boldsymbol{V}_m|}{\mathrm{d}z^2} = [\boldsymbol{T}_V]^{-1}[\boldsymbol{L}][\boldsymbol{C}][\boldsymbol{T}_V] \cdot \frac{\mathrm{d}^2|\boldsymbol{V}_m|}{\mathrm{d}t^2} \tag{8}$$

$$\frac{\mathrm{d}^2|\boldsymbol{I}_m|}{\mathrm{d}z^2} = [\boldsymbol{T}_I]^{-1}[\boldsymbol{C}][\boldsymbol{L}][\boldsymbol{T}_I] \cdot \frac{\mathrm{d}^2|\boldsymbol{I}_m|}{\mathrm{d}t^2} \tag{9}$$

where $|\boldsymbol{V}_m|$ and $|\boldsymbol{I}_m|$ are the vectors of modal voltages and currents at time t and distance z along the line, respectively. $[\boldsymbol{T}_V]$ and $[\boldsymbol{T}_I]$ are the square matrices of the eigenvectors.

The solution of the differential equation system in the phase domain takes the following form:

$$|\boldsymbol{I}(t)| = [\boldsymbol{G}_L] \cdot |\boldsymbol{V}(t)| - [\boldsymbol{T}_I] \cdot |\boldsymbol{I}_m(t - \tau_m)| \tag{10}$$

where $[\boldsymbol{G}_L]$ is a conductance matrix representing the couplings between phases, and τ_m is the modal travel time. The equivalent circuit is reported in Fig. 17, with reference to a generic node.

There is no analytical solution for the wave equation of a lossy transmission line in the time domain. The line losses can be represented in the above model only by externally connected lumped resistances.